

Phase induced localization transition

Tong Liu(刘通), Xingbo Wei(魏兴波), and Youguo Wang(王友国)

Citation: Chin. Phys. B, 2024, 33 (**10**): 107103. DOI: 10.1088/1674-1056/ad6a0b
Journal homepage: http://cpb.iphy.ac.cn; http://iopscience.iop.org/cpb

What follows is a list of articles you may be interested in

Topological phase transition in compressed van der Waals superlattice heterostructure BiTeCl/$HfTe_2$

Zhilei Li(李志磊), Yinxiang Li(李殷翔), Yiting Wang(王奕婷), Wenzhi Chen(陈文执), and Bin Chen(陈斌)
Chin. Phys. B, 2024, 33 (**8**): 087102. DOI: 10.1088/1674-1056/ad462e

Multi-objective global optimization approach predicted quasi-layered ternary TiOS crystals with promising photocatalytic properties

Yi-Jie Xiang(向依婕), Siyan Gao(高思妍), Chunlei Wang(王春雷), Haiping Fang(方海平), Xiangmei Duan(段香梅), Yi-Feng Zheng(郑益峰), and Yue-Yu Zhang(张越宇)
Chin. Phys. B, 2024, 33 (**8**): 087101. DOI: 10.1088/1674-1056/ad4bc3

Two-dimensional Sb net generated nontrivial topological states in $SmAgSb_2$ probed by quantum oscillations

Jian Yuan(袁健), Xian-Biao Shi(石贤彪), Hong Du(杜红), Tian Li(李田), Chuan-Ying Xi(郗传英), Xia Wang(王霞), Wei Xia(夏威), Bao-Tian Wang(王保田), Rui-Dan Zhong(钟瑞丹), and Yan-Feng Guo(郭艳峰)
Chin. Phys. B, 2024, 33 (**7**): 077102. DOI: 10.1088/1674-1056/ad4bc2

Unveiling the pressure-driven metal-semiconductor-metal transition in the doped TiS_2

Jiajun Chen(陈佳骏), Xindeng Lv(吕心邓), Simin Li(李思敏), Yaqian Dan(但雅倩), Yanping Huang(黄艳萍), and Tian Cui(崔田)
Chin. Phys. B, 2024, 33 (**6**): 067104. DOI: 10.1088/1674-1056/ad4325

Anisotropic metal-insulator transition in strained VO_2(B) single crystal

Zecheng Ma(马泽成), Shengnan Yan(闫胜楠), Zenglin Liu(刘增霖), Tao Xu(徐涛), Fanqiang Chen(陈繁强), Sicheng Chen(陈思成), Tianjun Cao(曹天俊), Litao Sun(孙立涛), Bin Cheng(程斌), Shi-Jun Liang(梁世军), and Feng Miao(缪峰)
Chin. Phys. B, 2024, 33 (**6**): 067103. DOI: 10.1088/1674-1056/ad39d4

Phase induced localization transition

Tong Liu(刘通)[1], Xingbo Wei(魏兴波)[2,†], and Youguo Wang(王友国)[1,‡]

[1] *School of Science, Nanjing University of Posts and Telecommunications, Nanjing* 210003, *China*
[2] *Department of Physics and Key Laboratory of Optical Field Manipulation of Zhejiang Province, Zhejiang Sci-Tech University, Hangzhou* 310018, *China*

(Received 31 May 2024; revised manuscript received 17 July 2024; accepted manuscript online 1 August 2024)

Localization phenomenon is an important research field in condensed matter physics. However, due to the complexity and subtlety of disordered systems, new localization phenomena always emerge unexpectedly. For example, it is generally believed that the phase of the hopping term does not affect the localization properties of the system, so the calculation of the phase is often ignored in the study of localization. Here, we introduce a quasiperiodic model and demonstrate that the phase change of the hopping term can significantly alter the localization properties of the system through detailed numerical simulations, such as the inverse participation ratio and multifractal analysis. This phase-induced localization transition provides valuable information for the study of localization physics.

Keywords: phase, localization, quasiperiodic

PACS: 71.23.Ft, 71.10.Fd, 71.23.An **DOI:** 10.1088/1674-1056/ad6a0b

1. Introduction

The concepts of topology and localization in condensed matter physics are pivotal areas of study, which reveal profound insights into the behavior of quantum systems.[1–3] Topological phenomena[4] in materials are characterized by global properties that remain unchanged under continuous deformations, providing a robust framework for understanding quantum states that are resistant to local perturbations. Localization,[5] on the other hand, refers to the phenomenon in which disorder within a system leads to spatial confinement of wave functions, significantly impacting the transport characteristics of electrons. The interaction between topology and localization not only enhances our theoretical comprehension but also lays the groundwork for practical applications in quantum computing and materials science. This interplay[6,7] is particularly fascinating because it is essential for the development of advanced technological devices. In addition, there are numerous exquisite toy models in the field, with the Harper–Hofstadter (HH) model[8] and Aubry–André–Harper (AAH) model[9,10] serving as archetypes of low-dimensional topological physics and localized physics, respectively.

The HH model, also known as the Hofstadter butterfly model, investigates the quantum behavior of electrons in a two-dimensional lattice subjected to a perpendicular magnetic field. The model,[8] initially proposed by Douglas Hofstadter in 1976, offers valuable insights into the behavior of electrons in magnetic fields and carries significant implications for the study of topological phases of matter and quantum computing.[11] In the HH model, electrons traverse a square lattice in which each lattice site represents an atom, allowing for electron hopping between sites. The presence of a perpendicular magnetic field introduces a phase factor to the hopping terms due to the magnetic vector potential, which is proportional to the magnetic flux through the lattice. The most remarkable characteristic of the HH model is its fractal energy spectrum, famously depicted as the Hofstadter butterfly.[12]

The AAH model studies the localization phenomena in quasiperiodic systems.[13,14] The model[9,10] introduced by S. Aubry and G. André in 1980 explores the transition between extended and localized states in a one-dimensional lattice with a quasiperiodic potential, which is intermediate between completely periodic and disordered systems. The self-duality of the AAH model is a significant aspect because it maintains invariance under a Fourier transform, exchanging the roles of position and momentum in the mathematical form of the Hamiltonian.[15,16] The AAH model not only enhances our comprehension of quasiperiodic systems but also acts as a link between the physics of ordered and disordered systems, providing a fertile area for exploration in both theoretical and experimental condensed matter physics.[17,18]

The primary connection between the HH and AAH models lies in their shared emphasis on the impact of competing periodicities.[19] The HH model explores the interaction between lattice periodicity and magnetic field periodicity, while the AAH model investigates the effects of quasiperiodicity. Both models provide valuable insights into phenomena such as Anderson localization and the quantum Hall effect,[20] illustrating the ways in which different scales and types of periodicity can impact electronic properties in disordered and externally magnetized systems. The hopping terms in the AAH model are characterized by zero phase factors, while

†Corresponding author. E-mail: weixingbo@zstu.edu.cn
‡Corresponding author. E-mail: wangyg@njupt.edu.cn

© 2024 Chinese Physical Society and IOP Publishing Ltd

the HH model can be effectively reduced to a one-dimensional AAH-like model with non-zero phase factors. The presence of non-zero phase factors significantly influences the topological properties of the HH model. In contrast, it is widely accepted that the phase factor has no impact on the localization properties of the AAH model or quasiperiodic systems.[21,22] A natural question arises: do phase factors have an impact on localization? In this study, we introduce a quasiperiodic system and demonstrate that the phase of the hopping terms can also significantly alter the localization properties of the system.

2. Model and results

Consider an exponentially decaying hopping model with a phase factor, characterized by the discrete Schrödinger equation

$$\sum_{l=1}^{\infty} \mathrm{e}^{p(1-l)}(\mathrm{e}^{-\mathrm{i}\theta}\psi_{n-l}+\mathrm{e}^{\mathrm{i}\theta}\psi_{n+l}) +2V\sum_{l=1}^{\infty}\mathrm{e}^{p(1-l)}\cos(2\pi\alpha l n)\psi_n = E\psi_n, \tag{1}$$

where $p>0$ represents the exponential decay parameter, V is the quasiperiodic potential strength, and ψ_n is the amplitude of wave function at the nth lattice, l takes positive integers. We choose the irrational number $\alpha=(\sqrt{5}-1)/2$. When the phase θ is set to 0, Eq. (1) becomes the quasiperiodic model studied in Ref. [23], which hosts a generalized duality symmetry and rich critical states. In this work, we focus on the $\theta\neq 0$ case.

To acquire the eigenvalue E and the associated wave functions ψ, we first numerically diagonalize the Schrödinger equation [Eq. (1)]. Then, it is convenient to calculate physical quantities through comprehensive numerical analysis. The localization of a wavefunction ψ can be determined by the inverse participation ratios,[24–26]

$$\mathrm{IPR}_j=\sum_{n=1}^{L}|\psi_n^{(j)}|^4, \tag{2}$$

where ψ has been normalized, L represents the total number of lattice sites, and j denotes the energy level index. Localized states are characterized by an IPR that is independent of the system size L due to their unaffected nature by boundaries. In contrast, extended states exhibit scaling with the system size, leading to corresponding IPRs that scale like L^{-1} and tend towards 0. While critical states demonstrate multifractality and are characterized by the scaling exponent between 0 and 1.

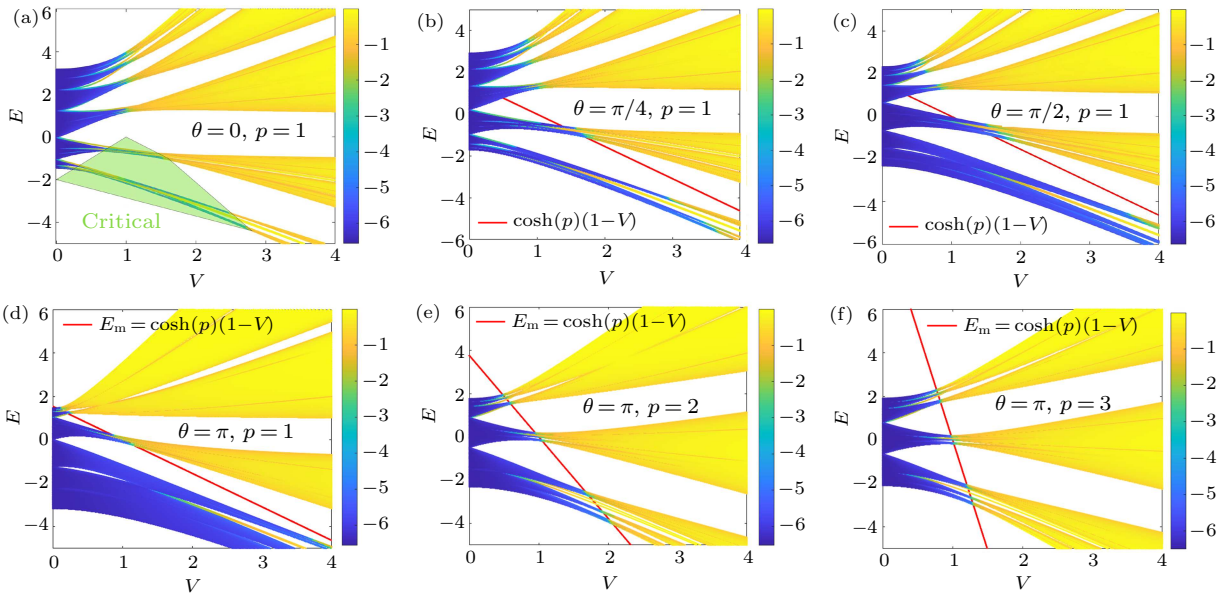


Fig. 1. The eigenvalues and log(IPR) of Eq. (1) as a function of V. Different colors of the eigenvalue curves indicate different magnitudes of log(IPR). The blue region denotes extended states and the yellow region denotes localized states. (a) When $\theta=0$ and $p=1$, the system has a large number of critical states, as seen in the green region, which is completely consistent with Ref. [23]. (b) and (c) When $0<\theta<\pi$ and $p=1$, there exists a delocalization-localization phase transition in the energy spectrum, but the phase boundary is not clearly defined. (d) When $\theta=\pi$ and $p=1$, the delocalization-localization phase boundary in the energy spectrum becomes clear and regular, the red solid line represents the estimated mobility edge $E_{\mathrm{m}}=\cosh(p)(1-V)$. Panels (e) and (f) illustrate that the estimated mobility edge is applicable to other p-values when $\theta=\pi$. The total number of sites is set to be $L=987$.

To highlight the distinction between extended, critical, and localized states, we analyze the IPR scaling exponent, log(IPR), instead of focusing solely on the raw value of the IPR. Figure 1 depicts the spectrum E of various parameters θ and p as a function of the quasiperiodic potential strength V, with consideration given to a system size of $L=987$. The color representation indicates the log(IPR) of the corresponding eigenvalues. Specifically, the blue region signifies that the corresponding eigenstates are extended. On the contrary, the yellow region indicates that the corresponding eigenstates are

localized. As depicted in Fig. 1(a), the spectrum of Eq. (1) [$\theta = 0$ and $p = 1$] is composed of multiple bands, for $E > 0$, the extended-localized transition point occurs at $V = 1$, while for $E < 0$, the transition point transforms into a critical region (green area). All of these numerical findings align well with the predictions in Ref. [23].

When $0 < \theta < \pi$ and $p = 1$, the spectrum of Eq. (1) undergoes a dramatic change, an irregular delocalization–localization phase transition occurs in the energy spectrum, as shown in Figs. 1(b) and 1(c). Surprisingly, when $\theta = \pi$ and $p = 1$, there is no extended-localized transition observed around $V = 1$, and the critical regions also disappear. Instead, a regular mobility edge emerges to delineate the boundary between extended and localized states, with the estimated expression for the mobility edge being $E_{\rm m} = \cosh(p)(1 - V)$, as shown in Fig. 1(d). To verify the robustness of the mobility edge, we conduct numerical simulations for various p-values and demonstrate that the estimated expression also fits very well, thus proving its robustness, as shown in Figs. 1(e) and 1(f). We have also explored alternative parameter combinations and found that except for $\theta = 0$ and π, all other values of θ have a corresponding pair with $\theta + \pi$, such as the localization properties of $\theta = \pi/2$ being the same as those of $\theta = 3\pi/2$. These numerical findings indicate that substantial changes in the system's localization occur as the phase of the hopping terms varies, a novel phenomenon not previously observed in studies on disordered systems.

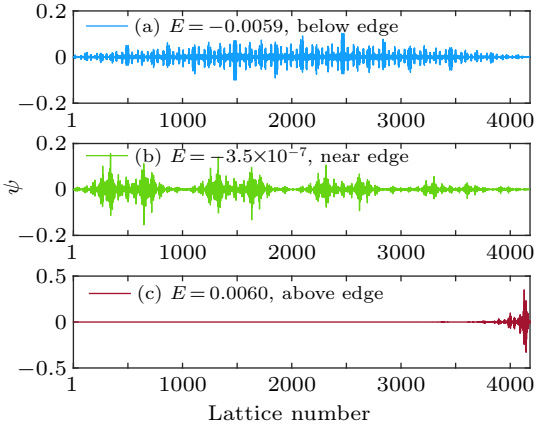


Fig. 2. Eigenstates numerically obtained from Eq. (1) [$\theta = \pi$] with $p = 1$, $V = 1$ and $L = 4181$, and the estimated mobility edge $E_{\rm m} = 0$. Three different eigenvalues: (a) low energy extended state below $E_{\rm m} = 0$, (b) critical state near $E_{\rm m} = 0$, and (c) high energy localized state above $E_{\rm m} = 0$.

To further confirm the presence of the mobility edge, we illustrate the spatial distributions of related eigenstates with eigenvalues close to $E_{\rm m}$. We specify the parameters $p = 1$, $V = 1$, and $L = 4181$ for performing the numerical calculation. We select three typical wave functions with corresponding eigenvalues that are above, below, and near the mobility edge $E_{\rm m} = 0$. Figure 2 illustrates the spatial distributions of different eigenstates. As depicted in Fig. 2(a), the eigenstate exhibits intuitive extension, with the corresponding eigenvalue below $E_{\rm m} = 0$. In Fig. 2(c), the eigenstate corresponds to localized states, with an eigenvalue above $E_{\rm m} = 0$. Notably, in Fig. 2(b), the eigenvalue is close to $E_{\rm m} = 0$, and the eigenstate clearly demonstrates self-similar properties, indicating that this state is neither fully localized nor extended over the entire space, namely, it is a critical state.

3. Criticality and multifractal analysis

The eigenstates at the mobility edge in the case of $\theta = \pi$ exhibit critical behavior, while in the case of $\theta = 0$, there is also a significant number of critical states in the region where $E < 0$. To better compare the localization properties of these two cases, we employ multifractal analysis[27,28] to calculate the eigenstate properties. Multifractal analysis expands upon the concept of fractals, which are geometric structures displaying self-similar patterns across different scales. This approach is particularly valuable in quasiperiodic systems, where scale-invariant properties are manifested.

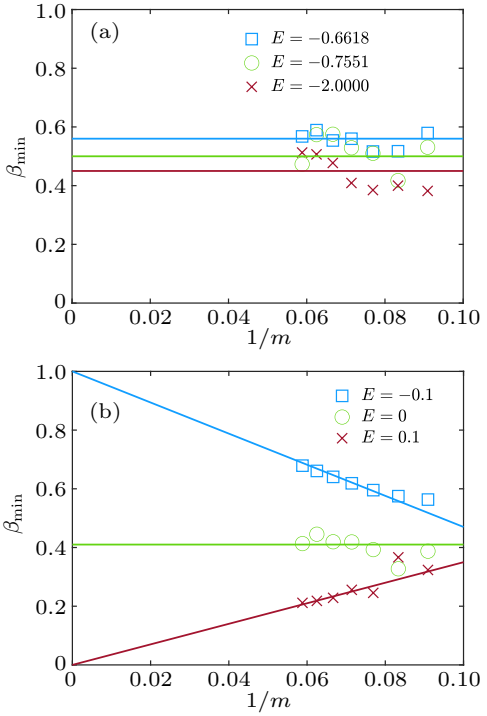


Fig. 3. (a) The $\beta_{\rm min}$ as a function of the inverse Fibonacci index $1/m$ for the $\theta = 0$ case. When $V = 1$ and $E < 0$, the eigenstates are critical states. (b) $\beta_{\rm min}$ as a function of the inverse Fibonacci index $1/m$ for the $\theta = \pi$ case. The green markers correspond to the critical state ($E = 0$), the blue markers correspond to the extended state ($E = -0.1$), and the red markers correspond to the localized state ($E = 0.1$).

For each wave function $\psi_n^{(j)}$, a scaling exponent $\beta_n^{(j)}$ can be derived from the nth probability $P_n^{(j)} = |\psi_n^{(j)}|^2 \sim (1/F_m)^{\beta_n^{(j)}}$. According to multifractal analysis, in the case of an extended eigenstate, the maximum of $P_n^{(j)}$ scales as $\max(P_n^{(j)}) \sim (1/F_m)^1$, indicating that $\min(\beta_n^{(j)}) = 1$. Conversely, for a localized eigenstate, $P_n^{(j)}$ peaks at a single lattice

and is close to zero at other lattices, resulting in $\max(P_n^{(j)}) \sim (1/F_m)^0$, or equivalently $\min(\beta_n^{(j)}) = 0$. As for critical eigenstates, the corresponding value of $\beta_{\min}^{(j)}$ falls within the interval $(0,\ 1)$ and can serve as a distinguishing factor between extended and localized states.

Figure 3 illustrates the dependence of $\beta_{\min}$ on the inverse Fibonacci index $1/m$. In Fig. 3(a), it is evident that for the case of $\theta = 0, V = 1$ and $E < 0$, $\beta_{\min}$ lies within the range $(0, 1)$ in the limit of large L, consistent with the findings in Fig. 1(a). As shown in Fig. 3(b), when $\theta = \pi$ and $E = 0$, $\beta_{\min}$ also remains within $(0, 1)$ for large L, indicating critical behavior near the mobility edge $E_{\rm m} = 0$. For an eigenvalue of $E = -0.1$, $\beta_{\min}$ approaches 1 as L becomes large, suggesting extended states. Conversely, for an eigenvalue of $E = 0.1$, $\beta_{\min}$ asymptotically tends to 0 as L increases, indicating localized states. We have also checked other combinations of parameters and obtained the same results as expected.

The above numerical results illustrate that altering the phase of the hopping term significantly impacts the localization properties of the system. Specifically, a critical region ($\theta = 0$) containing numerous critical states is transformed into a region with a mobility edge ($\theta = \pi$). This phenomenon can be referred to phase induced localization transition.

4. Summary

In summary, we present a quasiperiodic model incorporating the hopping phase, and thoroughly analyze the localization properties of this model. Our findings reveal that when the phase is set to 0, the system displays numerous critical states; conversely, setting the phase to π results in the appearance of a mobility edge that separates extended and localized states in the spectrum. This highlights the significant role of an initially overlooked phase in this system, leading to a remarkable change in its localization properties. Our findings reveal a new phenomenon in localized physics and lay the groundwork for further elucidating the underlying physical mechanisms.

Acknowledgements

Project supported by the National Natural Science Foundation of China (Grant No. 62071248), the Zhejiang Provincial Natural Science Foundation of China (Grant No. LQ24A040004), Natural Science Foundation of Nanjing University of Posts and Telecommunications (Grant No. NY223109), and China Postdoctoral Science Foundation (Grant No. 2022M721693).

References

[1] Qi X and Zhang S 2011 *Rev. Mod. Phys.* **83** 1057
[2] Kitaev A 2001 *Phys. Usp.* **44** 131
[3] Anderson P 1958 *Phys. Rev.* **109** 1492
[4] Ivanov D 2001 *Phys. Rev. Lett.* **86** 268
[5] Biddle J and Das Sarma S 2010 *Phys. Rev. Lett.* **104** 070601
[6] Jin L and Song Z 2019 *Phys. Rev. B* **99** 081103(R)
[7] Liu T and Cheng S 2023 *Chin. Phys. B* **32** 027102
[8] Hofstadter D 1976 *Phys. Rev. B* **14** 2239
[9] Aubry S and André G 1980 *Ann. Isr. Phys. Soc.* **3** 18
[10] Harper P 1955 *Proc. Phys. Soc. London Sect. A* **68** 874
[11] Jimenez-Garcia K, LeBlanc L, Williams R, Beeler M, Perry A and Spielman I 2012 *Phys. Rev. Lett.* **108** 225303
[12] Zhou L and Han W 2021 *Chin. Phys. B* **30** 100308
[13] Liu T, Guo H, Pu Y and Longhi S 2020 *Phys. Rev. B* **102** 024205
[14] Yao H, Khouldi H, Bresque L and Sanchez-Palencia L 2019 *Phys. Rev. Lett.* **123** 070405
[15] Liu T and Xia X 2024 *Chin. Phys. Lett.* **41** 017102
[16] Cai X, Lang L, Chen S and Wang Y 2013 *Phys. Rev. Lett.* **110** 176403
[17] Wei X, Gao X and Zhu W 2022 *Phys. Rev. B* **106** 134207
[18] Wei X, Cheng C, Gao X and Mondaini R 2019 *Phys. Rev. B* **99** 165137
[19] Chiu C, Teo J, Schnyder A and Ryu S 2016 *Rev. Mod. Phys.* **88** 035005
[20] Hatsugai Y 1993 *Phys. Rev. Lett.* **71** 3697
[21] Lang L, Cai X and Chen S 2012 *Phys. Rev. Lett.* **108** 220401
[22] Liu Y, Zhou Q and Chen S 2021 *Phys. Rev. B* **104** 024201
[23] Gonçalves M, Amorim B, Castro E and Ribeiro P 2023 *Phys. Rev. Lett.* **131** 186303
[24] Liu T, Xia X, Longhi S and Sanchez-Palencia L 2022 *SciPost Phys.* **12** 027
[25] Wei X, Wu L, Feng K, Liu T and Zhang Y 2024 *Phys. Rev. A* **109** 023314
[26] Cai X 2022 *Phys. Rev. B* **106** 214207
[27] Liu T, Cheng S, Zhang R, Ruan R and Jiang H 2022 *Chin. Phys. B* **31** 027101
[28] Hiramoto H and Kohmoto M 1989 *Phys. Rev. B* **40** 8225